

# Solution Nuclear Magnetic Resonance Spectroscopy Techniques for Probing Intermolecular Interactions

## Review

Maurizio Pellecchia\*

Cancer Research Center and  
Inflammation and Infectious Disease Center  
The Burnham Institute  
10901 North Torrey Pines Road  
La Jolla, California 92037

### Summary

Nuclear magnetic resonance (NMR) spectroscopy in solution has evolved into a powerful technique for structure determination of proteins and nucleic acids. More recently, a number of NMR-based approaches have been developed to monitor and characterize intermolecular interactions. These approaches offer unique advantages over other techniques and find their utility in both structural biology and drug discovery. We will report on basic principles and recent examples of the application of such NMR methodologies to characterize protein-protein interactions and for ligand binding studies and drug discovery.

### Introduction

In this manuscript, we wanted to reiterate some of the principles underlying nuclear magnetic resonance (NMR)-based techniques that enable the characterization of intermolecular interactions. Particular emphasis will be put on the characterization of protein-protein and protein-ligand interactions and their use in lead discovery and optimization. The bottom line in most of these experiments is that NMR parameters of either a protein target (or nucleic acid) or a ligand are different depending on whether the molecules are isolated in solution or form a complex. During the past several years, a number of techniques that are best suited to detect these differences have been developed. In essence, most of such techniques can be grouped into two main categories. In a first, “direct” approach, protein NMR observables are directly monitored in the presence of a binder (another macromolecule or a small molecule). A second approach is based on the so-called “transferred” techniques, in which the changes in nuclear spin relaxation of a protein or a small molecule are measured in the presence of a substoichiometric amount of target. In addition, we will report on methods to detect enzyme kinetics and inhibition, in which the consumption of a substrate or a cofactor, or the formation of an enzymatic product, is directly monitored by NMR. The main advantage of these strategies in the drug discovery process is that even weak binders or inhibitors can be detected, with a relatively lower incidence of false positives than any other type of assay. However, despite NMR laboratory automation, the use of compound mixtures and liquid handlers for sample preparation, NMR-based assays are intrinsically of a low-throughput nature due to the relatively large amounts of target

needed and the relatively lengthy experimental time. Hence, the obvious way to exploit such assays is to select and screen small, but diverse, libraries of compounds representing “drug-like” building blocks to identify preferential scaffolds. These initial, weak hits could subsequently be optimized by using a number of strategies. This so-called fragment-based approach to drug discovery [1–12] is becoming more and more popular given its versatility to tackle more complex systems for which high-throughput screening techniques are not as easily applicable, such as protein-protein interactions. We believe that the NMR-based techniques reported here will play an increasingly important role in chemical biology and target validation, particularly when dealing with “unconventional” and/or less characterized drug targets.

### NMR-Based Binding Studies that Rely on the Observation of Protein Resonances

#### *Macromolecular NMR Spectroscopy: A Brief History*

The evolution of NMR spectroscopy from an analytical technique into an alternative approach to X-ray crystallography in the determination of protein and nucleic acid conformation in solution became possible with the development of bidimensional [ $^1\text{H}$ ,  $^1\text{H}$ ] nuclear Overhauser effect spectroscopy (NOESY) [13]. In this key NMR experiment, short (<5 Å) internuclear distances between hydrogen nuclei can be measured and directly used to probe protein conformation in solution. This area of research evolved into the current field of modern macromolecular NMR spectroscopy in solution. In recognition of the tremendous impact of this line of research on the scientific community, Nobel Prizes in Chemistry were awarded “for [the] contributions to the development of the methodology of high-resolution nuclear magnetic resonance (NMR) spectroscopy” to Prof. Richard R. Ernst [14, 15] in 1991, and to Prof. Kurt Wüthrich in 2002 “for his development of nuclear magnetic resonance spectroscopy for determining the three-dimensional structure of biological macromolecules in solution” [16, 17]. In order to extend these basic principles and techniques to larger proteins (up to ~40 kDa), where the problem of resonance overlap in bidimensional NMR experiments becomes insurmountable, multidimensional and triple resonance experiments were introduced in the early 90s by Dr. Ad Bax (National Institutes of Health) [18–21], and soon after by several other investigators (reviewed in several references such as [22–25]). In these experiments, additional NMR observable nuclei such as  $^{15}\text{N}$  and  $^{13}\text{C}$  are exploited. For recombinant proteins that can be obtained from bacterial expression systems (mainly *E. coli*), enrichment of protein samples with these nuclei is now routine. In contrary, labeling proteins in other expression systems is still too pricey, but great steps in cell-free expression are being made [26]. By using 3D and 4D triple resonance experiments that exploit magnetization transfers between neighboring  $^1\text{H}$ ,  $^{15}\text{N}$ , and  $^{13}\text{C}$  nuclei, sequence-specific resonance assignments of

\*Correspondence: mpellecchia@burnham.org

proteins up to 30–40 kDa can be obtained. With the availability of the assignments for most hydrogen resonances in a protein, internuclear distances are subsequently measured via 3D or 4D versions of the 2D [ $^1\text{H}$ ,  $^1\text{H}$ ]-NOESY experiment, in which the additional dimensions can be either  $^{15}\text{N}$  or  $^{13}\text{C}$ , again to ameliorate the problem of resonance overlap. Following the strategies pioneered by Wüthrich and coworkers [27, 28], three-dimensional models of the protein that satisfy these distance constraints can be generated. Nowadays, iterative resonance assignments and refinements of the structure can be obtained semiautomatically, enormously reducing the time needed to obtain a structure by NMR spectroscopy (see, for example, [29–31]).

With the advent of protein labeling and heteronuclear protein NMR spectroscopy techniques, other studies become possible. Because nuclear spin relaxation mechanisms are strictly correlated with local motion, scientists started to realize that proteins' overall and internal motion can be accurately monitored by nuclear spin relaxation measurements. It turns out that protein mobility in solution is nonuniform, with a large variety of rates and types of dynamics. Investigators in several research laboratories are trying to find a correlation between this motion and functional aspects of protein folding and catalysis [22, 23, 32–34].

In the late 90s, another breakthrough in the field came with the development of the so-called TROSY (transverse relaxation optimized spectroscopy)-type techniques [35, 36]. In brief, the technique exploits simple nuclear spin relaxation physics principles to artificially increase the relaxation times of  $^{15}\text{N}$ ,  $^1\text{H}$ , and, in some instances,  $^{13}\text{C}$  nuclei, a phenomenon that has a maximum effect at higher magnetic fields. This results in increasing the resolution of macromolecular spectra and allows for the study of large macromolecular complexes in which rapid nuclear relaxation poses a serious obstacle.

Currently, the combination of advances in instrumentation, the use of orientational constraints in partially oriented media [37, 38], the use of selective  $^{13}\text{C}$ ,  $^1\text{H}$ -methyl labeling in otherwise deuterated samples [39, 40], the simultaneous acquisition of multidimensional experiments [41], the use of segmental labeling techniques [42–45], and the use of TROSY-type experiments have made NMR spectroscopy a very powerful and efficient tool for structural biology initiatives [46]. Finally, very recent developments in projection spectroscopy [47–51] enable the reconstruction of a full multidimensional spectrum by recording discrete sets of lower-dimension projection experiments. Combined with automated assignment strategies [52], this approach promises to significantly reduce the time needed for data collection and analysis.

It did not take much longer for scientists in both industry and academia to realize that NMR could also be very useful in monitoring intermolecular interactions involving other macromolecules or, in particular, a ligand (for recent reviews, see also, for example, [10, 53–56]). Much of the remainder of this article deals with this subject.

#### **Protein-Protein and Protein-Ligand Interactions: The Chemical Shift Mapping**

Let's consider the binding of a ligand L to a target macromolecule T by a two-site, second-order exchange

process (Equation 1):



In assessing the effects of chemical exchange on a NMR spectrum, the lifetime of a particular conformational state relates directly to selected NMR parameters. The lifetimes of the free states for the ligand L,  $\tau_L$ , and the target,  $\tau_T$ , can be expressed as functions of the populations,  $p$ , of the free and bound states:

$$\tau_L = p_L / (k_{\text{off}} * p_{\text{LT}}) \quad (2)$$

and

$$\tau_T = p_T / (k_{\text{off}} * p_{\text{TL}}), \quad (3)$$

where  $p_L = [\text{L}]/[\text{L}_0]$ ,  $p_T = [\text{T}]/[\text{T}_0]$ ,  $p_{\text{LT}} = [\text{TL}]/[\text{L}_0]$ , and  $p_{\text{TL}} = [\text{TL}]/[\text{T}_0]$ , with  $\text{L}_0$  and  $\text{T}_0$  representing the total concentrations of ligand and receptor, respectively.  $k_{\text{on}}$  and  $k_{\text{off}}$  represent the on- and off-rates, respectively, for the formation of the complex TL (see also Equation 6). For convenience in discussing exchange effects, a single lifetime is commonly defined as:

$$1/\tau = 1/\tau_L + 1/\tau_T = k_{\text{off}} * (1 + p_{\text{TL}}/p_L). \quad (4)$$

The relative magnitudes of the lifetime  $\tau$  and the inverse of the chemical shift differences between free and bound states will affect the appearance of the NMR spectrum of the protein in the presence of a ligand. In the system defined by Equation 1, separate resonance lines for the free and bound ligands will be observed if the exchange rate is slow on the “chemical shift timescale.” That is, if  $1/\tau$  is slower than the chemical shift difference between the resonances of the bound and free ligands in frequency units:

$$1/\tau < \Delta\delta, \quad (5)$$

where  $\Delta\delta = |(\delta_{\text{TL}} - \delta_L)|$ .

If the exchange rate is fast on the chemical shift timescale, the chemical shift mapping by stepwise titration can also provide a measurement of the dissociation constant ( $K_d$ ) by correlating the fractional chemical shift change with the total ligand concentration:

$$K_d = k_{\text{off}}/k_{\text{on}} = [\text{T}][\text{L}]/[\text{TL}] \quad (6)$$

At the equilibrium:  $[\text{TL}] = p\text{T}_0$ ,  $[\text{T}] = (1 - p)[\text{T}_0]$ , and  $[\text{L}] = [\text{L}_0] - p[\text{T}_0]$ . Introducing these relations into Equation 6, we obtain:

$$p = \frac{([\text{T}_0] + [\text{L}_0] + K_d) - \sqrt{([\text{T}_0] + [\text{L}_0] + K_d)^2 - 4[\text{L}_0][\text{T}_0]}}{2[\text{T}_0]} \quad (7)$$

The parameter  $p$  represents the fractional population of bound versus free species at equilibrium, which, for fast exchanging ligands, is measured as:

$$p = (\delta_{\text{obs}} - \delta_{\text{free}}) / (\delta_{\text{sat}} - \delta_{\text{free}}) \quad (8)$$

$\delta_{\text{obs}}$  is the observed receptor chemical shift during the titration, and  $\delta_{\text{free}}$  and  $\delta_{\text{sat}}$  are the chemical shifts for the receptor in the unbound and fully bound (saturated) states, respectively.  $K_d$  can then be determined by a nonlinear least squares fit of  $p$  versus  $[\text{L}_0]$ . If we use  $K_d$  values to estimate  $k_{\text{off}}$  values, ligands that bind with dissociation constants greater than  $10^{-5}$  M will be in

the fast exchange limit for chemical shift timescales, if we assume a diffusion controlled on-rate of  $\sim 10^8\text{--}10^9\text{ M}^{-1}\text{s}^{-1}$ . Those in the  $10^{-6}\text{--}10^{-7}\text{ M}$  range often fall into the intermediate range between the slow and fast exchange limiting situations, and those at  $10^{-8}\text{ M}$  or smaller are usually in the slow exchange limit.

A simple technique that exploits differences in chemical shift between free and bound protein targets is based on the detection of such changes in  $^{15}\text{N}/^1\text{H}$  and/or  $^{13}\text{C}/^1\text{H}$  correlation spectra of a protein (or nucleic acid) upon titration of a ligand or a mixture of ligands. Chemical shift mapping can also provide crude structural information on the site of binding when the resonance assignments are known. Nowadays, collection of  $[^{15}\text{N}, ^1\text{H}]$  or  $[^{13}\text{C}, ^1\text{H}]$  correlations spectra (either TROSY-type or conventional heteronuclear multiple quantum correlation and heteronuclear single quantum correlation) with uniformly or amino acid-type selectively labeled protein samples are the methods of choice [57–65]. In analyzing chemical shift perturbation data, care must be taken that long-range effects due to conformational changes are possible. In such cases, differential chemical shift mapping by comparing spectra of complexes between the target and two slightly different ligands have been proposed [59, 66, 67].

Measurements of chemical shift perturbation can also be used to map interactions between macromolecules provided that a differential labeling can be engineered (Figure 1A). In this approach, a protein domain (or nucleic acid) is studied by NMR in the context of a larger macromolecular complex. For example, the complex between the molecular chaperone FimC and the pilus subunit FimH (>50 kDa) could be studied by  $[^{15}\text{N}, ^1\text{H}]$ -TROSY experiments by using a sample containing  $^{15}\text{N}/^2\text{H}$ -labeled FimC and unlabeled FimH (Figure 1B) [68]. The surface of FimC interacting with FimH could be mapped, and the binding site could be delineated. When the X-ray structure of the complex was subsequently obtained [69], it confirmed the NMR-determined site of interaction between the two proteins (Figure 1B).

The use of chemical shift mapping to monitor ligand binding has several major advantages. First, binders to a given protein can be found without the need of developing a specific assay or even regardless of the knowledge of its function. This is generally true for most of the NMR-based techniques. In addition, given that the resonance assignments are known, the location of the site of binding can be obtained. Moreover, if the structure of the target was previously determined by NMR, in some instances it is possible to rapidly derive intermolecular NOE-type constraints to precisely locate the ligand on the protein binding site. The drawback of the chemical shift mapping is that the amount of protein needed for a single NMR experiment has to be relatively high for the technique to be used efficiently to test large libraries of compounds. However, we have to emphasize again that the technique is also very sensitive to weak binding events, a fact that is largely exploited in most of the NMR-based drug discovery strategies. When such a weak binder (or preferred scaffold) is found to bind to a given protein, follow-up hit optimizations strategies can be devised to iteratively increase the affinity of the compound.

A clever application of the chemical shift mapping is

the SAR (structure-activity relationships) by NMR strategy [63, 65]. Here, a chemical shift mapping-based screen for a second binder is performed in the presence of an initial weak hit (Figures 1C and 1D). Compounds that induce chemical shift changes that correspond to a region on the protein surface that is adjacent to the site of binding of the first ligand are considered. The structural characterization of the ternary complex by NMR allows for the design of potential chemical linkers between the compounds to afford a more potent ligand, according the Equation 9:

$$K_D^{AB} = K_D^A * K_D^B * E, \quad (9)$$

where  $K_D^{AB}$  is the dissociation constant for the bidentate compound,  $K_D^A$  and  $K_D^B$  are the dissociation constants of the individual initial binders, and  $E$  is the linking coefficient [63]. In terms of free energy of binding:

$$\Delta G^{AB} = \Delta H^A + \Delta H^B - T\Delta S^{AB} = -RT \ln K_D^{AB}, \quad (10)$$

where  $R$  is the Boltzman constant,  $T$  is the temperature of the system,  $\Delta H^A$  and  $\Delta H^B$  are the enthalpy of binding of ligand A and ligand B, respectively, and  $\Delta S^{AB}$  represents the entropy loss upon binding of the bidentate compound. In an ideal case, this latter value could be approximated to equal the loss of entropy of binding of the isolated compounds (A or B). In other words, the binding affinity of the bidentate compound is, in principle, higher than that of the individual compounds because of a larger number of interactions (enthalpy factor), but also because of a reduced loss in entropy upon binding. In practice, however, attaining perfectly rigid linkers that allow for the simultaneous binding of A and B is not always possible, and, inevitably, disturbance in the binding of individual compounds can be introduced by the linker itself. Nevertheless, the approach has been demonstrated to yield bidentate compounds with dramatically increased affinity with respect to the individual fragments [63] (Figure 1D; see also Figure 4B and “Transferred Effects”). In practical applications, initial bidentate compounds represent the starting point for traditional SAR-based optimizations to obtain even more potent and selective compounds (for a recent example, see [70]).

### Transferred Effects

Let's consider a system of two dipolarly coupled spins, I and S (two hydrogen nuclei). The time evolution of the longitudinal relaxation of the individual spins is given by the Solomon equations [71]:

$$d\langle I_z \rangle / dt = -\rho_I(\langle I_z \rangle - I_0) - \sigma_{IS}(\langle S_z \rangle - S_0) \quad (11)$$

$$d\langle S_z \rangle / dt = -\rho_S(\langle S_z \rangle - S_0) - \sigma_{IS}(\langle I_z \rangle - I_0). \quad (12)$$

$\rho$  and  $\sigma_{IS}$  represent the auto-relaxation and crossrelaxation rates, and  $I_0$ ,  $S_0$ ,  $\langle I_z \rangle$ , and  $\langle S_z \rangle$  are the equilibrium and transient magnetization components of spins I and S. Saturation of spin I, with  $\langle I_z \rangle = 0$ , results in the following expression for the steady-state situation ( $d\langle S_z \rangle / dt = 0$ ):

$$\langle S_z \rangle = S_0 + (\sigma_{IS}/\rho)I_0. \quad (13)$$

Assuming that I and S are like spins (protons in most applications), the saturation of I changes the intensity

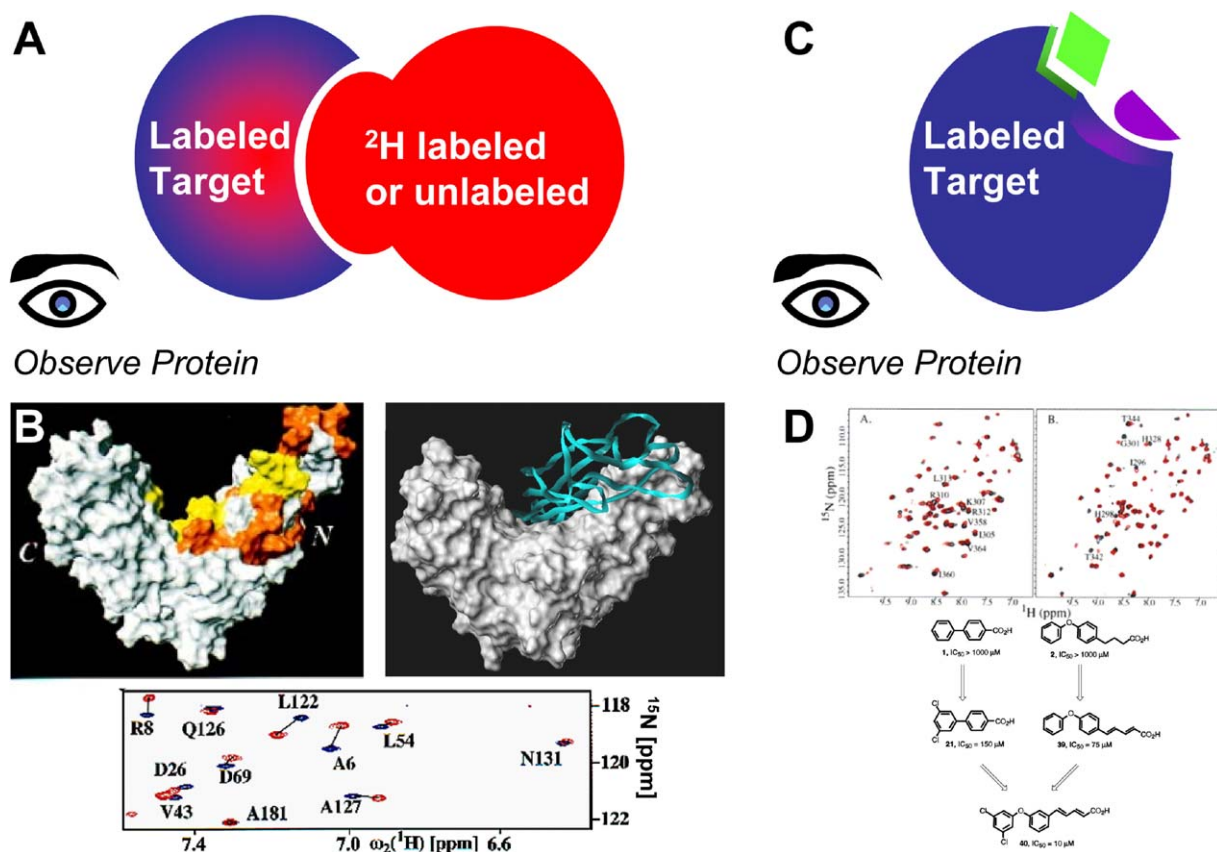


Figure 1. Monitoring Intermolecular Interactions via Chemical Shift Perturbation Measurements

(A) Schematic representation of chemical shift mapping.

(B) The mapping of the pilus chaperone FimC (23 kDa,  $^{15}\text{N}/^2\text{H}$ -labeled in 90:10  $\text{H}_2\text{O}:\text{D}_2\text{O}$  buffer) for the pilus subunit FimH (28 kDa) monitored via  $^{15}\text{N}$ ,  $^1\text{H}$ -TROSY (a region of the spectra is shown: red, bound; black, apo). The differences in chemical shifts between apo and bound FimC are mapped on the 3D NMR structure of FimC (left) and are highlighted on the surface of FimC in orange (large shifts), yellow (smaller shifts), and white (no shifts). Reproduced from [68]. As a comparison, on the right is reported the X-ray structure of the complex between FimC (surface representation, in white) and FimH (ribbon representation). The area identified by the mapping strategy coincides with the region of interaction that was later identified by X-ray crystallography.

(C and D) Schematic representation of the SAR by NMR approach and an example of a small bidentate molecule designed by using this approach. Reproduced from [95].

of the S resonance by  $(\sigma_{\text{IS}}/\rho)$  relative to the equilibrium value, producing what is referred to as the “steady-state NOE” [17].

The manifestation of the NOE is a function of the nuclear spin crossrelaxation rates that are in turn linked to the molecular correlation time. Small molecules tumble very rapidly in solution, leading to positive NOEs: the saturation of a nucleus induces a maximum relative signal increase of  $\sim 10\%$  on adjacent nuclei. Macromolecules (or a small molecule bound to a macromolecule) tumble slowly, resulting in negative NOEs: the saturation of a given nucleus results in a signal decrease in adjacent nuclei, with a maximum effect of  $-100\%$ . Let's introduce at this point an important consideration about a small molecule binder at equilibrium with a larger macromolecule. In analogy with slow and fast exchange in the chemical shift timescale discussed in the previous paragraph, we can have slow or fast exchange in the relaxation timescales. Slow exchange occurs when the rate of equilibration,  $1/\tau$ , is slower than the

difference of the longitudinal and transverse relaxation rates (denoted with  $R_1$  and  $R_2$ , respectively) of the small molecules in the free versus the bound state:

$$1/\tau \ll |(R_{2,\text{TL}} - R_{2,\text{L}})| \text{ and/or } 1/\tau \ll |(R_{1,\text{TL}} - R_{1,\text{L}})|. \quad (14)$$

Likewise, fast exchange occurs if the rate of equilibration,  $1/\tau$ , is faster than the difference in relaxation rates:

$$1/\tau \gg |(R_{2,\text{TL}} - R_{2,\text{L}})| \text{ and/or } 1/\tau \gg |(R_{1,\text{TL}} - R_{1,\text{L}})|. \quad (15)$$

An important consequence of Equation 15 is that, in the fast exchange regime, the relaxation properties of a ligand at equilibrium with its complex with a macromolecular target is the weight average between the values corresponding to the free and fully bound states.

In such situations (for ligands or macromolecular binders in the low-micromolar to millimolar binding af-



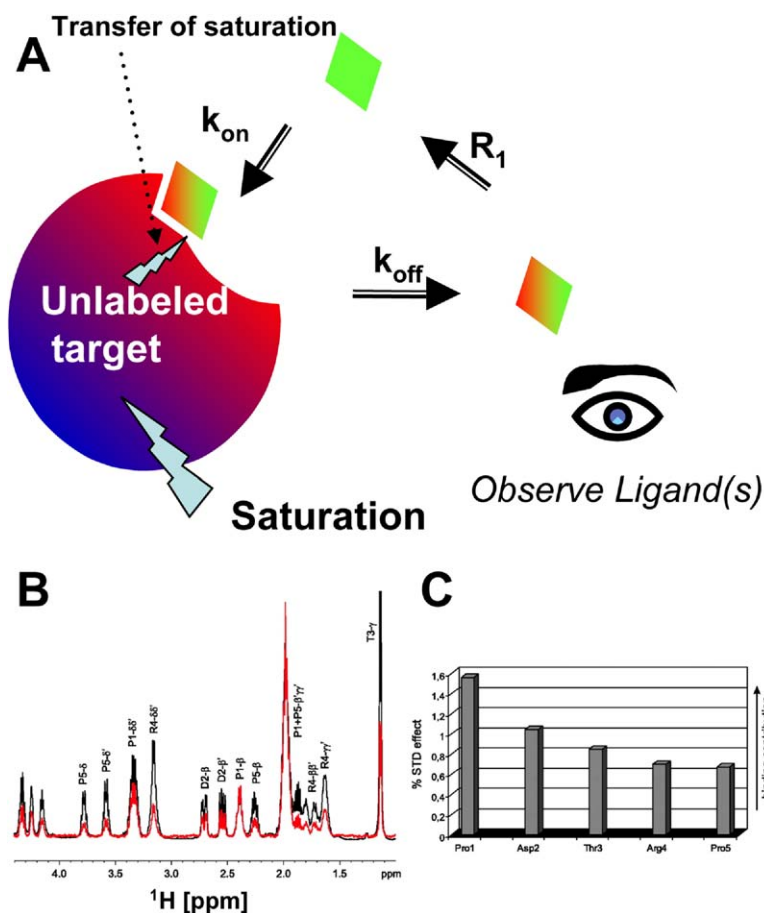


Figure 2. Monitoring Ligand-Protein Interactions via Saturation Transfer Measurements

(A) Schematic representation of the saturation transfer difference (STD) experiment.

(B) Example of a typical STD experiment illustrating the spectrum of the peptide PDTRP recorded in the presence of the antibody SM3 with a presaturation of the aliphatic region with a train of selective pulses. The difference spectrum was obtained by comparison with the same spectrum recorded by placing the irradiation well outside the spectral window of both the target and the small molecule (red spectrum). The 1D spectrum of the peptide is also shown (black), and the intensity is adjusted so that the Pro1-β-methylene signal is the same height in both spectra.

(C) Relative saturation of each resonance line of the compound. This information can be correlated to the mode of binding of a given ligand. Reproduced from [74].

inities), ligand binding can then be detected by measuring the relaxation properties of the ligand in the presence of a substoichiometric amount of target.

In the saturation transfer difference (STD) experiment [72, 73], a 1D steady-state NOE experiment is measured for a ligand in the presence of a small amount of target, usually at a ligand:protein ratio of about 100:1. As is illustrated in Figure 2A, when  $R_1$  (the longitudinal relaxation rate for the proton nuclei of the small molecule) is longer than the  $k_{off}$  of the complex, there will be an accumulation of saturated ligand if the target is also present in a substoichiometric amount. The experiment is based on a selective saturation of protein resonances by irradiating regions of the  $^1\text{H}$  NMR spectrum (for example the aliphatic region of the spectrum, between -1 and 2 ppm) that are usually not occupied by resonances from small organic molecules. Subsequently, a difference spectrum is generated from two spectra that are recorded with and without preirradiation of protein resonances. In the example reported in Figure 2, the spectrum of the peptide PDTRP is recorded in the presence of the antibody SM3 with a presaturation of the aliphatic region with a train of selective pulses. The difference spectrum can be obtained by comparison with the same spectrum recorded by placing the train of pulses well outside the spectral window of both the target and the small molecule (Figure 2B, red spectrum). As a comparison, the 1D spectrum of the peptide is

also shown (Figure 2B, black spectrum), and the intensity is adjusted so that the Pro1-β-methylene signal is the same height in both spectra. Clearly visible is a strong STD effect for protons of Pro1 and Asp2, whereas the signals of Arg4 and Pro5 are less affected by the saturation of the antibody resonances [74]. The STD amplification factor (Equation 16) [75] is the fractional saturation of a given proton multiplied by the excess of the ligand over the protein and was introduced to allow for a better assessment of the absolute magnitude of the STD effect:

$$\text{STD amplification factor} = (I_0 - I_{\text{sat}})/I_0 \times \text{ligand excess.} \quad (16)$$

In Equation 16,  $(I_0 - I_{\text{sat}})/I_0$  is the fractional STD effect, expressing the signal intensity in the STD spectrum as a fraction of the intensity of an unsaturated reference spectrum.

The STD amplification factor provides an easy measure to quantify the amplification of the protein information observed in the STD signals of the ligand and can be used to compare the STD effect of the corresponding resonances of the two molecules in the competition or titration experiments, even if the protein concentration is not identical in the corresponding NMR samples.

From the relative saturation of the resonance lines within a given binder (Figure 2C), the epitope of the interactions can be obtained.

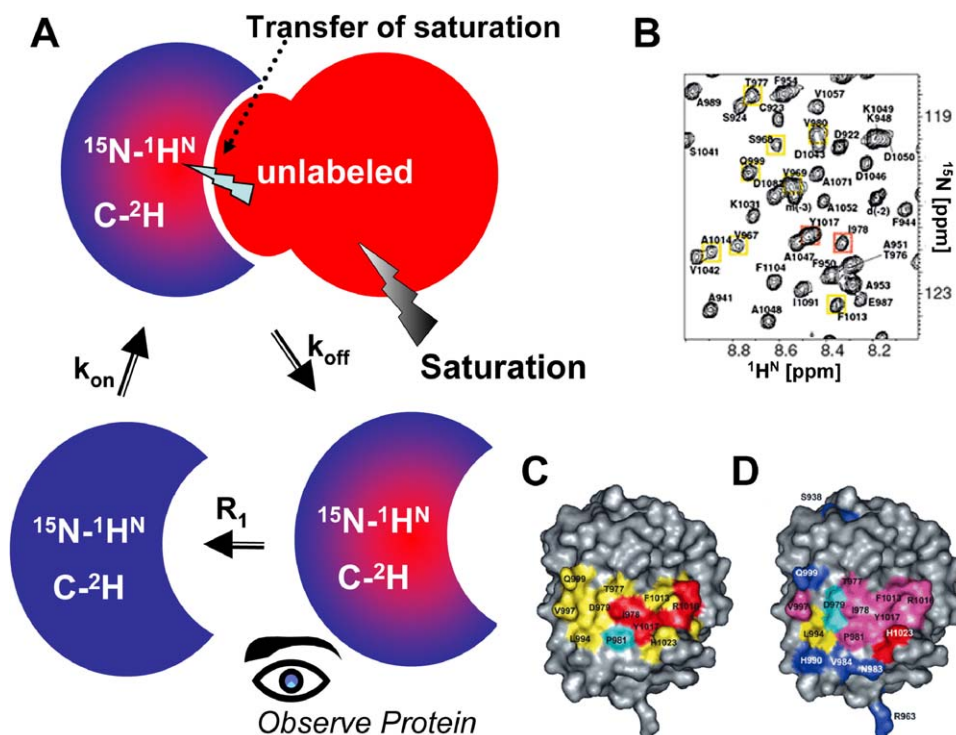


Figure 3. Monitoring Protein-Protein Interactions via Differential Labeling and Transfer of Saturation

(A) Schematic representation of the saturation transfer in the characterization of protein-protein interactions. One protein is labeled with  $^{15}\text{N}$  and deuterated everywhere, except for the amides, which can be exchanged to protons in  $\text{H}_2\text{O}$  buffer. The second protein is unlabeled. Therefore, the saturation of the aliphatic region of the spectrum of a sample constituted by the two interacting proteins corresponds to a selective saturation of the unlabeled protein.

(B) Example of mapping protein surfaces via saturation transfer. The intensity of crosspeaks in a  $[\text{}^{15}\text{N}, \text{}^1\text{H}]$ -TROSY experiment measured with  $^{15}\text{N}/^2\text{H}$ -labeled A3 domain in the presence of a small amount of immobilized collagen type III is measured with a presaturation centered at the aliphatic region of the spectrum (therefore saturating collagen resonances) or outside the spectral region (as reference).

(C and D) The decrease of intensities between the two spectra is mapped into the 3D structure of the A3 domain and compared in (D) with single point mutations that have been found to be important for binding to the A3 domain for collagen type III. Reproduced from [78].

WaterLOGSY (Water Ligand Observation by Gradient Spectroscopy) is a related experiment in which the selective saturation of the protein is achieved indirectly by irradiation of water protons [76]; however, the experiment is not suitable for epitope mapping.

As in the case of chemical shift mapping, transferred effects could also be used to monitor macromolecular interactions provided that a differential labeling scheme could be obtained (Figure 3A). In an application that is essentially similar to the STD approach described above, the interaction between two proteins is monitored by the acquisition of  $[\text{}^{15}\text{N}, \text{}^1\text{H}]$ -TROSY NMR spectra of a protein target, which is deuterated in all nonexchangeable protons (Figure 3A). Two spectra are recorded in the presence of a substoichiometric amount of the second unlabeled protein (again, at about a 100:1 molar ratio), with and without saturation of the aliphatic regions of the spectrum (Figures 3A and 3B) [77]. Because the second protein is unlabeled and the first one is deuterated, the saturation of hydrogen nuclei in the aliphatic region of the spectrum corresponds to a selective saturation of the unlabeled protein. The saturation is then transferred to the amide-protons of the interacting protein via the NOE and is detected via

TROSY-NMR (Figures 3A and 3B). Provided that  $R_1$  (the longitudinal relaxation rate for the amide protons of the labeled protein) is longer than the  $k_{\text{off}}$  of the complex, there will be an accumulation of saturated protein even if the unlabeled partner protein is present in a substoichiometric amount (Figures 3A and 3B). In the example reported in Figure 3, this method was used to map the interactions between a  $^{15}\text{N}/^2\text{H}$ -labeled A3 domain and type III collagen [78]. The transfer of saturation, when mapped into the 3D structure of the A3 domain (Figure 3C), identifies residues that had been previously found by single point mutations to be important for binding to the A3 domain for collagen type III, as highlighted in Figure 3D.

Another example of a transferred experiment that can be used to detect ligand binding is the 2D  $[\text{}^1\text{H}, \text{}^1\text{H}]$ -NOESY spectrum. When measured for a small molecule in the presence of a small amount of protein target, it gives very strong negative intramolecular NOEs (diagonal and crosspeaks will have the same sign) or very small positive NOEs (very weak crosspeaks of opposite signs with respect to the diagonal peaks), depending on whether the compound does or does not bind to the target, respectively.

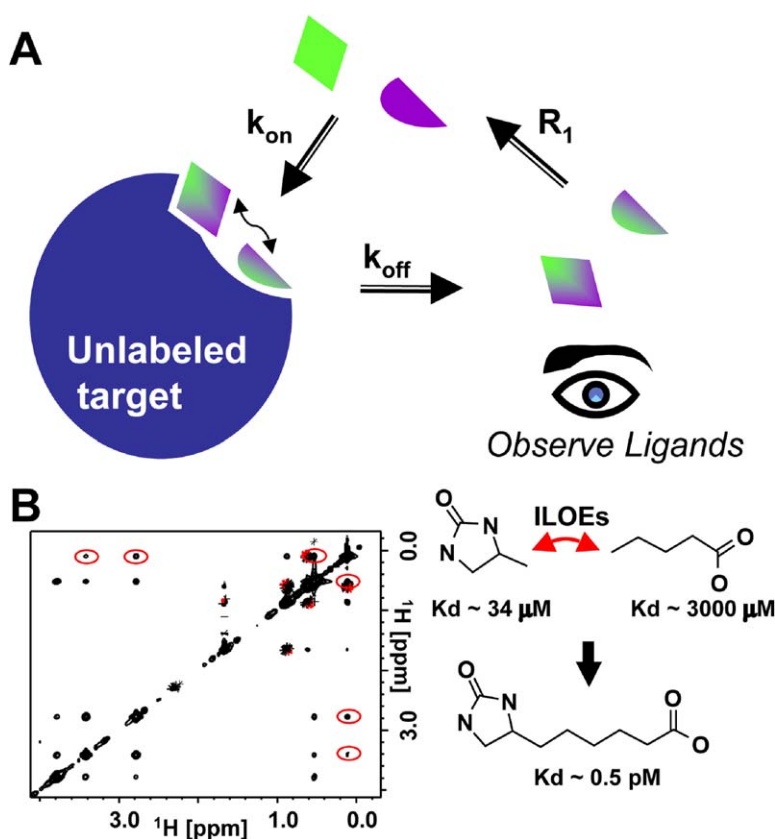


Figure 4. Protein-Mediated Ligand-Ligand Magnetization Transfer

(A) Schematic representation of the ligand-ligand NOE experiment (ILOE). Provided that  $R_{1A}$  and  $R_{1B}$  (the longitudinal relaxation rates for the protons of both ligands) are longer than their individual  $k_{off}$  rates for the target, ligand-ligand magnetization transfer can be observed for the two ligands if also in the presence of a substoichiometric amount of protein target. For the ILOEs to be present, the largest distance between the two protons, each on one of the proximal ligands, should be  $<5 \text{ \AA}$ .

(B) Example of protein-mediated ligand-ligand NOEs, between *n*-pentanoic acid and 4-methylimidazolidin-2-one, measured in the presence of a substoichiometric amount of Avidin. Ligand-ligand NOEs are indicated with red circles. Reproduced from [80].

These techniques are often referred to as based on “transferred” effects because the relaxation effects induced on the ligand by the target are transferred to the free ligand [79].

In addition to intramolecular NOEs, the observation of protein-mediated ligand-ligand NOEs (ILOEs) [53, 59, 60, 80–84] can be extremely informative in the design of potential bidentate compounds and for lead optimization. Please note again that unlike direct, protein-based NMR experiments, the ILOEs between adjacent compounds are only mediated by the protein that is therefore needed only in small amounts and unlabeled (Figure 4A). Also, in this case, the size of the protein is not a limiting factor. Even larger proteins are preferred given that the ILOEs intensities are greater for slow-tumbling molecules [53]. In an application we called SAR by ILOEs, in analogy to the SAR by NMR method, the design of potential bidentate compounds can be achieved via detection of ILOEs in compound mixtures [83]. To enhance the crossrelaxation rates of the bound compounds, protein fusions can be used such as GST fusion constructs [53]. These will have an artificially increased molecular weight. In fact, when we used this technique for smaller proteins ( $<15 \text{ kDa}$ ), the intensity of the ILOE crosspeaks decreased dramatically. This strategy can also be used to design selectivity, where only fragments that uniquely bind (even weakly) to a given protein target are used for lead optimization [80–82]. In the example reported in Figure 4B, two weakly binding compounds derived from fragmenting the compound desthiobiotin (a ligand for the protein Avidin with

picomolar affinity) display intramolecular and intermolecular NOEs (ILOEs) in the presence of a substoichiometric amount of Avidin. Clearly, the potent binder desthiobiotin could have been designed based on the observation of ligand-ligand NOEs between the two fragments despite their low affinities (Figure 4), demonstrating the power of the approach [80]. In another recent example, we designed and synthesized a series of compounds that binding to the surface of the proapoptotic protein Bid, preventing its interactions with the mitochondrial membrane [53]. This is an example of a protein that could not have been easily targeted with “conventional” screening techniques. Because high-affinity ligands could in principle be designed and synthesized against targets with unknown structure or even less characterized function, this approach should be very powerful not only in lead discovery and optimization projects, but also in reverse chemical-genetics studies, in which the discovered high-affinity binders can be used to determine the eventual phenotypic alterations that they induce in a cellular context [85].

#### Other Techniques

Fast exchange in the relaxation timescales also works in enhancing the transverse relaxation times of a ligand when in contact with a substoichiometric amount of target. In a first application, ligand screening can be achieved by measuring a 1D  $^1H$  NMR spectrum of the ligand(s) with a relaxation filter (a spin-lock) in the presence and absence of a substoichiometric amount of target. The relaxation filter has two functions: first, it

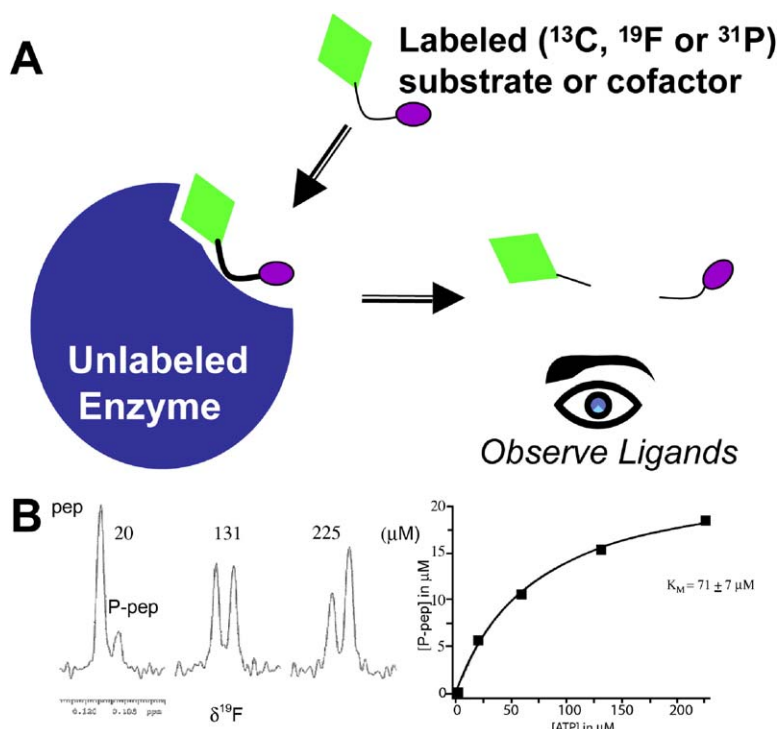


Figure 5. Monitoring Enzyme Kinetics and Inhibition by NMR

(A) Schematic representation of the detection of enzyme kinetics by NMR.

(B) Measurements of protein kinase B activity by using a peptide of sequence  $\text{CF}_3\text{-CO-ARKRERAYSFGHHA}$ . The two peaks correspond to the nonphosphorylated peptide and the one in which the Ser residue is phosphorylated. Reproduced from [92].

eliminates any residual signal from the target; second, it enhances the differences in intensities between binders and nonbinders. In typical applications, ligands can be tested in mixtures at concentrations as low as  $50 \mu\text{M}$ , and in the presence of a target concentration as low as  $1 \mu\text{M}$  [86]. Another approach to artificially enhance the transverse relaxation of a ligand upon binding is to introduce a paramagnetic spin on the target. If the target contains a metal ion, the paramagnetic center could simply be the metal ion itself (e.g.,  $\text{Mn}^{2+}$ ) [59]. For other targets, a paramagnetic spin can be artificially introduced. A common spin label is 2,3,4,6-tetramethylpiperidine-1-oxyl (known as TEMPO) [87]. Finally, a second site screen could be obtained by labeling the first ligand with a spin label and using its relaxation enhancement effect to search for compounds that bind on the surface of the target in proximity to the first molecule. In analogy to the SAR by NMR and SAR by ILOEs approaches, this strategy would lead to a pair of compounds that occupy adjacent sites on the protein surface. While the drawback of the method is that a spin-labeled compound has to be obtained, the advantage of this method is that the protein is simply mediating the interactions. Hence, only small amounts of unlabeled target are needed, and the size of the target is not a limiting factor [88].

Another recent application of NMR for screening compounds makes use of an immobilized target [89]. In this approach, the immobilized protein is used to capture binders that exhibit a reduced signal intensity compared to a reference spectrum in which the ligand is exposed to the matrix alone. The advantages of such a technique over the transferred methods listed above are that a single sample can be used several times and

that even very strong binders (or those in slow exchange on the relaxation and chemical shift timescales) can be detected. An optimal use of this strategy is anticipated when combined with flow techniques [89].

#### Monitoring Enzyme Kinetics and Inhibition by NMR

Assay miniaturization and the development of more and more sensitive and reliable readouts have made the use of spectrophotometric assays the method of choice in detecting enzymatic activity. These methods have completely obscured one of the most obvious ways in which to use NMR spectroscopy in the drug discovery process: monitoring enzyme kinetics and inhibition. There are several reported cases in which NMR was found to be useful in specific applications; however, the application of general NMR-based enzymatic assays has remained sporadic until very recently, when more general applications to phosphatases, dehydrogenases, and two different classes of proteases have been reported [53, 90–92] (Figure 5A). The simple experimental schemes take advantage of  $^{31}\text{P}$  and  $^{19}\text{F}$  NMR in appropriately labeled substrates or cofactors. Observation of these nuclei offers two particular benefits: the large chemical shift dispersion and the high sensitivity of the chemical shift to even small differences in the chemical environment. Also, because these nuclei are relatively uncommon biologically, the observed spectra will not suffer from overlap with other signals from the reaction buffers.

In Figure 5, we report an example of a clever assay developed to detect enzyme kinetics and inhibition of protein kinase B by using a  $-\text{CF}_3$ -labeled peptide substrate [91]. The inhibition and the kinetic constants can be easily measured in the NMR tube (Figure 5B).



Such assays could be very useful when dealing with protein kinases [91], for example, where traditional assays for measuring phosphorylation of a reference peptide require the use of specific antibodies or radioactive ATP. Other cases in which having a simple NMR-based assay is useful include the characterization of inhibitors that may have an intrinsically high fluorescence or absorbance and, in fragment-based approaches, where compounds are tested at high concentrations while screening for preferential inhibitory scaffolds [53]. Small-molecule compounds may have several unexpected effects on the assay components. Therefore, even for the most reliable assays, having an orthogonal simple validation method such as the NMR assay is highly recommended. For example, when dealing with potential Caspase inhibitors [90], we have encountered compounds that have high fluorescence that we could not have reliably tested in the traditional fluorimetric assay. Other compounds could show activity in the fluorescence-based assay simply by aggregating the substrate peptide, a phenomenon that could simply be detected in the NMR-based assay, given that both cleaved and uncleaved substrates are observable.

A straightforward application of these types of assays is to monitor the inhibition propensities of small libraries of scaffolds (or fragments), tested at high concentration. Subsequent follow-up optimizations can follow the routes of medicinal chemistry and/or analog selection, possibly aided by virtual docking of large libraries of compounds containing the selected scaffold [53, 90]. Another recent example comes from our laboratories in which a  $^{19}\text{F}$ -based assay was devised to monitor the inhibitory properties of a small library of scaffolds against the protease LF from *B. anthracis*. Iterative optimizations of the initial micromolar inhibitor lead to a potent and selective compound [93]. Another powerful application of the NMR-based enzymatic assays occurs in functional screening projects, as recently reported by Dalvit and coworkers [94].

### Conclusions and Outlook

Current research efforts are focused on the discovery and validation of novel potential drug targets. The combination of bioinformatics, genome sequencing, and structural biology initiatives can generate a number of potential targets. NMR spectroscopy is a technique that has been playing a significant role in the structural elucidation of such protein targets, especially in the determination of the structure of protein domains in solution. However, the use of differential labeling and the advent of TROSY-type techniques have provided an additional dimension for the use of NMR in the structural biology field: the identification and characterization of macromolecular interfaces. The early identification of key interaction sites between macromolecular complexes by using either direct or transferred NMR-based approaches described above could rapidly provide information on possible targeting sites in the absence of atomic resolution X-ray structures of the complex. Moreover, NMR also has an important role in the study and characterization of the interactions between small organic molecules and macromolecular targets, and it is particularly useful in lead identification and optimiza-

tion processes. We anticipate a significant role of NMR-based techniques in the near future, especially at the early stages of target identification and validation and in the development of small, organic molecules capable of antagonizing complex macromolecular interactions.

### Acknowledgments

Several approaches and many elegant applications have been reported in the past years on the use of NMR spectroscopy in the drug discovery process and in monitoring protein-protein interactions. The paragraph on the history of macromolecular NMR spectroscopy only briefly describes this very rich and dynamic field of research. The author apologizes if he was unable to properly mention all of this work within the limited space of this article. This work was supported in part by National Institutes of Health grants P01 AI055789, U01 AI061139, and P01 CA102583.

Received: May 18, 2005

Revised: August 8, 2005

Accepted: August 25, 2005

Published: September 23, 2005

### References

1. Carr, R.A., Congreve, M., Murray, C.W., and Rees, D.C. (2005). Fragment-based lead discovery: leads by design. *Drug Discov. Today* 10, 987–992.
2. Congreve, M., Carr, R., Murray, C., and Jhoti, H. (2003). A 'rule of three' for fragment-based lead discovery? *Drug Discov. Today* 8, 876–877.
3. Erlanson, D.A., and Hansen, S.K. (2004). Making drugs on proteins: site-directed ligand discovery for fragment-based lead assembly. *Curr. Opin. Chem. Biol.* 8, 399–406.
4. Erlanson, D.A., McDowell, R.S., and O'Brien, T. (2004). Fragment-based drug discovery. *J. Med. Chem.* 47, 3463–3482.
5. Erlanson, D.A., Wells, J.A., and Braisted, A.C. (2004). Tethering: fragment-based drug discovery. *Annu. Rev. Biophys. Biomol. Struct.* 33, 199–223.
6. Gill, A., Cleasby, A., and Jhoti, H. (2005). The discovery of novel protein kinase inhibitors by using fragment-based high-throughput X-ray crystallography. *ChemBioChem* 6, 506–512.
7. Hartshorn, M.J., Murray, C.W., Cleasby, A., Frederickson, M., Tickle, I.J., and Jhoti, H. (2005). Fragment-based lead discovery using X-ray crystallography. *J. Med. Chem.* 48, 403–413.
8. Moore, W.R., Jr. (2005). Maximizing discovery efficiency with a computationally driven fragment approach. *Curr. Opin. Drug Discov. Devel.* 8, 355–364.
9. Rees, D.C., Congreve, M., Murray, C.W., and Carr, R. (2004). Fragment-based lead discovery. *Nat. Rev. Drug Discov.* 3, 660–672.
10. Schade, M., and Oschkinat, H. (2005). NMR fragment screening: tackling protein-protein interaction targets. *Curr. Opin. Drug Discov. Devel.* 8, 365–373.
11. Villar, H.O., Yan, J., and Hansen, M.R. (2004). Using NMR for ligand discovery and optimization. *Curr. Opin. Chem. Biol.* 8, 387–391.
12. Zartler, E.R., and Shapiro, M.J. (2005). Fragonomics: fragment-based drug discovery. *Curr. Opin. Chem. Biol.* 9, 366–370.
13. Kumar, A., Ernst, R.R., and Wüthrich, K. (1980). A two-dimensional nuclear Overhauser enhancement (2D NOE) experiment for the elucidation of complete proton-proton cross-relaxation network in biological macromolecules. *Biochem. Biophys. Res. Commun.* 95, 1–6.
14. Bo, M.G. (1997). Nobel Lectures in Chemistry 1991–1995 (Singapore: World Scientific Publishing Company).
15. Ernst, R.R., Bodenhausen, G., and Wokaun, A. (1987). Principles of Nuclear Magnetic Resonance in One and Two Dimensions (New York: Oxford University Press).
16. Wüthrich, K. (2003). NMR studies of structure and function of biological macromolecules. *Biosci. Rep.* 23, 119–168.

17. Wüthrich, K. (1986). *NMR of Proteins and Nucleic Acids* (New York: Wiley & Son).
18. Ikura, M., Kay, L.E., and Bax, A. (1990). A novel approach for sequential assignment of  $^1\text{H}$ ,  $^{13}\text{C}$ , and  $^{15}\text{N}$  spectra of proteins: heteronuclear triple-resonance three-dimensional NMR spectroscopy. Application to calmodulin. *Biochemistry* 29, 4659–4667.
19. Kay, L.E., Ikura, M., Tschudin, R., and Bax, A. (1990). 3-dimensional triple-resonance NMR-spectroscopy of isotopically enriched proteins. *J. Magn. Res.* 89, 496–514.
20. Bax, A., and Ikura, M. (1991). An efficient 3D NMR technique for correlating the proton and  $^{15}\text{N}$  backbone amide resonances with the alpha-carbon of the preceding residue in uniformly  $^{15}\text{N}/^{13}\text{C}$  enriched proteins. *J. Biomol. NMR* 1, 99–104.
21. Grzesiek, S., Dobeli, H., Gentz, R., Garotta, G., Labhardt, A.M., and Bax, A. (1992).  $^1\text{H}$ ,  $^{13}\text{C}$ , and  $^{15}\text{N}$  NMR backbone assignments and secondary structure of human interferon- $\gamma$ . *Biochemistry* 31, 8180–8190.
22. Gardner, K.H., and Kay, L.E. (1998). The use of  $^2\text{H}$ ,  $^{13}\text{C}$ ,  $^{15}\text{N}$  multidimensional NMR to study the structure and dynamics of proteins. *Annu. Rev. Biophys. Biomol. Struct.* 27, 357–406.
23. Kay, L.E. (1997). NMR methods for the study of protein structure and dynamics. *Biochem. Cell Biol.* 75, 1–15.
24. Pelton, J.G., and Wemmer, D.E. (1995). Heteronuclear NMR pulse sequences applied to biomolecules. *Annu. Rev. Phys. Chem.* 46, 139–167.
25. Whitehead, B., Craven, C.J., and Waltho, J.P. (1997). Double and triple resonance NMR methods for protein assignment. *Methods Mol. Biol.* 60, 29–52.
26. Ozawa, K., Headlam, M.J., Schaeffer, P.M., Henderson, B.R., Dixon, N.E., and Otting, G. (2004). Optimization of an *Escherichia coli* system for cell-free synthesis of selectively N-labelled proteins for rapid analysis by NMR spectroscopy. *Eur. J. Biochem.* 271, 4084–4093.
27. Williamson, M.P., Havel, T.F., and Wüthrich, K. (1985). Solution conformation of proteinase inhibitor IIA from bull seminal plasma by  $^1\text{H}$  nuclear magnetic resonance and distance geometry. *J. Mol. Biol.* 182, 295–315.
28. Wagner, G., Braun, W., Havel, T.F., Schaumann, T., Go, N., and Wüthrich, K. (1987). Protein structures in solution by nuclear magnetic resonance and distance geometry. The polypeptide fold of the basic pancreatic trypsin inhibitor determined using two different algorithms, DISGEO and DISMAN. *J. Mol. Biol.* 196, 611–639.
29. Guntert, P. (2004). Automated NMR structure calculation with CYANA. *Methods Mol. Biol.* 278, 353–378.
30. Zheng, D., Huang, Y.J., Moseley, H.N., Xiao, R., Aramini, J., Swapna, G.V., and Montelione, G.T. (2003). Automated protein fold determination using a minimal NMR constraint strategy. *Protein Sci.* 12, 1232–1246.
31. Herrmann, T., Guntert, P., and Wüthrich, K. (2002). Protein NMR structure determination with automated NOE-identification in the NOESY spectra using the new software ATNOS. *J. Biomol. NMR* 24, 171–189.
32. Schwalbe, H., Carlomagno, T., Hennig, M., Junker, J., Reif, B., Richter, C., and Griesinger, C. (2001). Cross-correlated relaxation for measurement of angles between tensorial interactions. *Methods Enzymol.* 338, 35–81.
33. Wüthrich, K. (1981). Nuclear magnetic resonance studies of internal mobility in globular proteins. *Biochem. Soc. Symp.* 46, 17–37.
34. Kern, D., and Züderweg, E.R. (2003). The role of dynamics in allosteric regulation. *Curr. Opin. Struct. Biol.* 13, 748–757.
35. Pervushin, K., Riek, R., Wider, G., and Wüthrich, K. (1997). Attenuated T2 relaxation by mutual cancellation of dipole-dipole coupling and chemical shift anisotropy indicates an avenue to NMR structures of very large biological macromolecules in solution. *Proc. Natl. Acad. Sci. USA* 94, 12366–12371.
36. Pervushin, K. (2000). Impact of transverse relaxation optimized spectroscopy (TROSY) on NMR as a technique in structural biology. *Q. Rev. Biophys.* 33, 161–197.
37. Bax, A. (2003). Weak alignment offers new NMR opportunities to study protein structure and dynamics. *Protein Sci.* 12, 1–16.
38. Prestegard, J.H., Bougault, C.M., and Kishore, A.I. (2004). Residual dipolar couplings in structure determination of biomolecules. *Chem. Rev.* 104, 3519–3540.
39. Goto, N.K., Gardner, K.H., Mueller, G.A., Willis, R.C., and Kay, L.E. (1999). A robust and cost-effective method for the production of Val, Leu, Ile ( $\delta$  1) methyl-protonated  $^{15}\text{N}$ -,  $^{13}\text{C}$ -,  $^2\text{H}$ -labeled proteins. *J. Biomol. NMR* 13, 369–374.
40. Kay, L.E., and Gardner, K.H. (1997). Solution NMR spectroscopy beyond 25 kDa. *Curr. Opin. Struct. Biol.* 7, 722–731.
41. Szyperki, T., Yeh, D.C., Sukumaran, D.K., Moseley, H.N., and Montelione, G.T. (2002). Reduced-dimensionality NMR spectroscopy for high-throughput protein resonance assignment. *Proc. Natl. Acad. Sci. USA* 99, 8009–8014.
42. Cowburn, D., and Muir, T.W. (2001). Segmental isotopic labeling using expressed protein ligation. *Methods Enzymol.* 339, 41–54.
43. Cowburn, D., Shekhtman, A., Xu, R., Ottesen, J.J., and Muir, T.W. (2004). Segmental isotopic labeling for structural biological applications of NMR. *Methods Mol. Biol.* 278, 47–56.
44. Romanelli, A., Shekhtman, A., Cowburn, D., and Muir, T.W. (2004). Semisynthesis of a segmental isotopically labeled protein splicing precursor: NMR evidence for an unusual peptide bond at the N-extein-intein junction. *Proc. Natl. Acad. Sci. USA* 101, 6397–6402.
45. Zuger, S., and Iwai, H. (2005). Intein-based biosynthetic incorporation of unlabeled protein tags into isotopically labeled proteins for NMR studies. *Nat. Biotechnol.* 23, 736–740.
46. Hol, W.G. (2000). Structural genomics for science and society. *Nat. Struct. Biol.* 7 (Suppl), 964–966.
47. Kupce, E., and Freeman, R. (2003). Projection-reconstruction of three-dimensional NMR spectra. *J. Am. Chem. Soc.* 125, 13958–13959.
48. Kupce, E., and Freeman, R. (2003). Reconstruction of the three-dimensional NMR spectrum of a protein from a set of plane projections. *J. Biomol. NMR* 27, 383–387.
49. Kupce, E., and Freeman, R. (2003). Fast multi-dimensional Hadamard spectroscopy. *J. Magn. Reson.* 163, 56–63.
50. Kupce, E., and Freeman, R. (2004). Projection-reconstruction technique for speeding up multidimensional NMR spectroscopy. *J. Am. Chem. Soc.* 126, 6429–6440.
51. Kupce, E., and Freeman, R. (2004). Fast reconstruction of four-dimensional NMR spectra from plane projections. *J. Biomol. NMR* 28, 391–395.
52. Hiller, S., Fiorito, F., Wüthrich, K., and Wider, G. (2005). Automated projection spectroscopy (APSY). *Proc. Natl. Acad. Sci. USA* 102, 10876–10881.
53. Pellecchia, M., Becattini, B., Crowell, K.J., Fattorusso, R., Forino, M., Fragai, M., Jung, D., Mustelin, T., and Tautz, L. (2004). NMR-based techniques in the hit identification and optimisation processes. *Expert Opin. Ther. Targets* 8, 597–611.
54. Lepre, C.A., Moore, J.M., and Peng, J.W. (2004). Theory and applications of NMR-based screening in pharmaceutical research. *Chem. Rev.* 104, 3641–3676.
55. Moore, J., Abdul-Manan, N., Fejzo, J., Jacobs, M., Lepre, C., Peng, J., and Xie, X. (2004). Leveraging structural approaches: applications of NMR-based screening and X-ray crystallography for inhibitor design. *J. Synchrotron Radiat.* 11, 97–100.
56. Johnson, M.A., and Pinto, B.M. (2004). NMR spectroscopic and molecular modeling studies of protein-carbohydrate and protein-peptide interactions. *Carbohydr. Res.* 339, 907–928.
57. Clarkson, J., and Campbell, I.D. (2003). Studies of protein-ligand interactions by NMR. *Biochem. Soc. Trans.* 31, 1006–1009.
58. Rodriguez-Mias, R.A., and Pellecchia, M. (2003). Use of selective Trp side chain labeling to characterize protein-protein and protein-ligand interactions by NMR spectroscopy. *J. Am. Chem. Soc.* 125, 2892–2893.
59. Pellecchia, M., Meininger, D., Dong, Q., Chang, E., Jack, R., and Sem, D.S. (2002). NMR-based structural characterization of large protein-ligand interactions. *J. Biomol. NMR* 22, 165–173.
60. Pellecchia, M., Sem, D.S., and Wüthrich, K. (2002). NMR in drug discovery. *Nat. Rev. Drug Discov.* 1, 211–219.
61. Sem, D.S., Bertolaet, B., Baker, B., Chang, E., Costache, A.D., Coutts, S., Dong, Q., Hansen, M., Hong, V., Huang, X., et al.

- (2004). Systems-based design of bi-ligand inhibitors of oxidoreductases: filling the chemical proteomic toolbox. *Chem. Biol.* **11**, 185–194.
62. Pellecchia, M., Meininger, D., Shen, A.L., Jack, R., Kasper, C.B., and Sem, D.S. (2001). SEA-TROSY (solvent exposed amides with TROSY): a method to resolve the problem of spectral overlap in very large proteins. *J. Am. Chem. Soc.* **123**, 4633–4634.
63. Shuker, S.B., Hajduk, P.J., Meadows, R.P., and Fesik, S.W. (1996). Discovering high-affinity ligands for proteins: SAR by NMR. *Science* **274**, 1531–1534.
64. Hajduk, P.J., Augeri, D.J., Mack, J., Mendoza, R., Yang, J., Betz, S.F., and Fesik, S.W. (2000). NMR-based screening of proteins containing <sup>13</sup>C-labeled methyl groups. *J. Am. Chem. Soc.* **122**, 7898–7904.
65. Hajduk, P.J., Sheppard, G., Nettesheim, D.G., Olejniczak, E.T., Shuker, S.B., Meadows, R.P., Steinman, D.H., Carrera, G.M., Marcotte, P.A., Severin, J., et al. (1997). Discovery of potent nonpeptide inhibitors of stromelysin using SAR by NMR. *J. Am. Chem. Soc.* **119**, 5818–5827.
66. Medek, A., Hajduk, P.J., Mack, J., and Fesik, S.W. (2000). The use of differential chemical shifts for determining the binding site location and orientation of protein-bound ligands. *J. Am. Chem. Soc.* **122**, 1241–1242.
67. McCoy, M.A., and Wyss, D.F. (2002). Structures of protein-protein complexes are docked using only NMR restraints from residual dipolar coupling and chemical shift perturbations. *J. Am. Chem. Soc.* **124**, 2104–2105.
68. Pellecchia, M., Sebbel, P., Hermanns, U., Wüthrich, K., and Glockshuber, R. (1999). Pilus chaperone FimC-adhesin FimH interactions mapped by TROSY-NMR. *Nat. Struct. Biol.* **6**, 336–339.
69. Choudhury, D., Thompson, A., Stojanoff, V., Langermann, S., Pinkner, J., Hultgren, S.J., and Knight, S.D. (1999). X-ray structure of the FimC-FimH chaperone-adhesin complex from uropathogenic *Escherichia coli*. *Science* **285**, 1061–1066.
70. Olthoff, T., Elmore, S.W., Shoemaker, A.R., Armstrong, R.C., Augeri, D.J., Belli, B.A., Bruncko, M., Deckwerth, T.L., Dinges, J., Hajduk, P.J., et al. (2005). An inhibitor of Bcl-2 family proteins induces regression of solid tumours. *Nature* **435**, 677–681.
71. Solomon, I. (1955). Relaxation processes in a system of two spins. *Phys. Rev.* **99**, 559–565.
72. Mayer, M., and Meyer, B. (1999). Characterization of ligand binding by saturation transfer difference NMR spectroscopy. *Ang. Chem. Int. Ed.* **38**, 1784–1788.
73. Klein, J., Meinecke, R., Mayer, M., and Meyer, B. (1999). Detecting binding affinity to immobilized receptor proteins in compound libraries by HR-MAS STD NMR. *J. Am. Chem. Soc.* **121**, 5336–5337.
74. Moller, H., Serttas, N., Paulsen, H., Burchell, J.M., Taylor-Papadimitriou, J., and Meyer, B. (2002). NMR-based determination of the binding epitope and conformational analysis of MUC-1 glycopeptides and peptides bound to the breast cancer-selective monoclonal antibody SM3. *Eur. J. Biochem.* **269**, 1444–1455.
75. Mayer, M., and Meyer, B. (2001). Group epitope mapping by saturation transfer difference NMR to identify segments of a ligand in direct contact with a protein receptor. *J. Am. Chem. Soc.* **123**, 6108–6117.
76. Dalvit, C., Pevarello, P., Tato, M., Veronesi, M., Vulpetti, A., and Sundstrom, M. (2000). Identification of compounds with binding affinity to proteins via magnetization transfer from bulk water. *J. Biomol. NMR* **18**, 65–68.
77. Takahashi, H., Nakanishi, T., Kami, K., Arata, Y., and Shimada, I. (2000). A novel NMR method for determining the interfaces of large protein-protein complexes. *Nat. Struct. Biol.* **7**, 220–223.
78. Nishida, N., Sumikawa, H., Sakakura, M., Shimba, N., Takahashi, H., Terasawa, H., Suzuki, E.I., and Shimada, I. (2003). Collagen-binding mode of vWF-A3 domain determined by a transferred cross-saturation experiment. *Nat. Struct. Biol.* **10**, 53–58.
79. Clore, G.M., and Gronenborn, A.M. (1983). Theory of the time-dependent transferred nuclear Overhauser effect - applications to structural analysis of ligand-protein complexes in solution. *J. Magn. Reson.* **53**, 423–442.
80. Kline, A. (1997). SAR by NOE? The NMR Newsletter **13**, 472.
81. Li, D., DeRose, E.F., and London, R.E. (1999). The inter-ligand Overhauser effect: a powerful new NMR approach for mapping structural relationships of macromolecular ligands. *J. Biomol. NMR* **15**, 71–76.
82. Fejzo, J., Lepre, C.A., Peng, J.W., Bemis, G.W., Murcko, M.A., and Moore, J.M. (1999). The SHAPES strategy: an NMR-based approach for lead generation in drug discovery. *Chem. Biol.* **6**, 755–769.
83. Becattini, B., Sareth, S., Zhai, D., Crowell, K.J., Leone, M., Reed, J.C., and Pellecchia, M. (2004). Targeting apoptosis via chemical design: inhibition of bid-induced cell death by small organic molecules. *Chem. Biol.* **11**, 1107–1117.
84. Driggers, E.M., Liu, C.W., Wemmer, D.E., and Schultz, P.G. (1998). Structure of the Michaelis complex of an efficient antibody acyl transferase determined by transferred nuclear Overhauser enhancement spectroscopy. *J. Am. Chem. Soc.* **120**, 1945–1958.
85. Becattini, B., and Pellecchia, M. (2005). SAR by ILOEs: an NMR-based approach to reverse chemical genetics. *Chem. Eur. J.* **11**, in press. 10.1002/chem.2005.00.636.
86. Hajduk, P.J., Olejniczak, E.T., and Fesik, S.W. (1997). One-dimensional relaxation- and diffusion-edited NMR methods for screening compounds that bind to macromolecules. *J. Am. Chem. Soc.* **119**, 12257–12261.
87. Jahnke, W., Rudisser, S., and Zurini, M. (2001). Spin label enhanced NMR screening. *J. Am. Chem. Soc.* **123**, 3149–3150.
88. Jahnke, W., Lawrence, B., Perez, L., Paris, G., Strauss, A., Fendrich, G., and Nalin, C.M. (2000). Second-site NMR screening with a spin-labeled first ligand. *J. Am. Chem. Soc.* **122**, 7394–7395.
89. Vanwetswinkel, S., Heetebrij, R.J., van Duynhoven, J., Holander, J.G., Filippov, D.V., Hajduk, P.J., and Siegal, G. (2005). TINS, target immobilized NMR screening: an efficient and sensitive method for ligand discovery. *Chem. Biol.* **12**, 207–216.
90. Fattorusso, R., Jung, D., Crowell, K.J., Forino, M., and Pellecchia, M. (2005). Discovery of a novel class of reversible non-peptide caspase inhibitors via a structure-based approach. *J. Med. Chem.* **48**, 1649–1656.
91. Dalvit, C., Fagerness, P.E., Hadden, D.T., Sarver, R.W., and Stockman, B.J. (2003). Fluorine-NMR experiments for high-throughput screening: theoretical aspects, practical considerations, and range of applicability. *J. Am. Chem. Soc.* **125**, 7696–7703.
92. Dalvit, C., Ardini, E., Flocco, M., Fogliatto, G.P., Mongelli, N., and Veronesi, M. (2003). A general NMR method for rapid, efficient, and reliable biochemical screening. *J. Am. Chem. Soc.* **125**, 14620–14625.
93. Forino, M., Johnson, S., Wong, T.Y., Rozanov, D.V., Savinov, A.Y., Li, W., Fattorusso, R., Becattini, B., Orry, A.J., Jung, D., et al. (2005). Efficient synthetic inhibitors of anthrax lethal factor. *Proc. Natl. Acad. Sci. USA* **102**, 9499–9504.
94. Dalvit, C., Ardini, E., Fogliatto, G.P., Mongelli, N., and Veronesi, M. (2004). Reliable high-throughput functional screening with 3-FABS. *Drug Discov. Today* **9**, 595–602.
95. Hajduk, P.J., Dinges, J., Miknis, G.F., Merlock, M., Middleton, T., Kempf, D.J., Egan, D.A., Walter, K.A., Robins, T.S., Shuker, S.B., et al. (1997). NMR-based discovery of lead inhibitors that block DNA binding of the human papillomavirus E2 protein. *J. Med. Chem.* **40**, 3144–3150.